nzsee
NEW ZEALAND SOCIETY FOR EARTHQUAKE ENGINEERING

Developing hysteresis curves for the optimised sliding hinge joint with asymmetric friction connections

J.T. Togher, C.J. Speirs & G.C. Clifton
Department of Civil and Environmental Engineering, University of Auckland, Auckland.

S. Ramhormozian
Built Environment Engineering Department, Auckland University of Technology, Auckland.

ABSTRACT

The semi-rigid Sliding Hinge Joint (SHJ) beam-column connection for steel moment resisting frames is a successful low damage system that shows a lot of promise in earthquake engineering. It allows for relative beam-column rotation during ULS shaking due to the sliding of the asymmetric friction connection (AFC). To further this connection, there has been a focus on developing mathematical representations of the hysteresis curves generated by the joint for use in seismic Time History Analyses (THA) of buildings in severe earthquakes. From the connections original form, the performance of the SHJAFC has been optimised with the use of partially compressed Belleville Springs. However, the initial mathematical representations of the hysteresis curves did not capture the improved behaviour of the optimised joint. The aim of the research is to take the displacement data of the optimised SHJ, then accurately predict the sliding force acting on the connection, thus presenting the updated moment-curvature relationship. To predict the sliding forces, a large set of statements are used. The statements determine where the current data point is in its hysteretic loop, what type of loading is acting upon it, and then predicts the force of the next data point. Once complete, representative curves can be made for different SHJs being acted upon by different displacements. This code could potentially be implemented into structural engineering open source software's to better understand the connection.

1 INTRODUCTION

Over the past decade, the sliding hinge joint (SHJ) has been under continual development to create a truly low-damage joint that works effectively in a moment resisting frame (MRF). The low-damage philosophy is to construct structures that can be occupied immediately after an ultimate limit state (ULS) event and to have the possibility of occupation after a large seismic event (MacRae, Clifton, & Innovations, 2013).This

philosophy has become common place after the Northridge (Hamburger & Frank, November 1994) and Kobe (Engelhardt, 2001) earthquakes which saw unprecedented damage to MRFs. Semi-rigid connections, such as SHJ, are at the forefront of the philosophy as the connections can achieve the criteria explained while simultaneously requiring minimal repairs. The lack of repairs aids in providing a cost-effective option in both post-earthquake usage and limited reinstating costs.

The type of semi-rigid connection that the SHJ falls under is called a slotted bolt connection (SBC). These are connections which contain clamped-by-bolt plates where bolts are present to allow for sliding and frictional resistance along the plate surface. The asymmetric friction connections (AFCs) contained within the SHJ, works by having the slotted holes in the bottom flange and web plates while leaving the top flange pinned. This allows for the rotation of the beam relative to the column through sliding of the AFCs.

Currently, the SHJ is widely used in New Zealand for MRSFs and has shown promising performance. There has been continual research into the connection to better learn its behaviour and capabilities. The most recent development has been the inclusion of Belleville Springs (BeSs) to retain bolt tension in the SHJ after a large seismic event and to improve its seismic performance such as increasing its self-centring tendency. BeSs are conical shaped washer springs which can compress and expand under movement and loading. The aims of the inclusion of the research into BeSs (Ramhormozian, Clifton, MacRae, Davet, & Khoo, 2019) were based around finding what caused the AFC bolt tension loss issue, whether different assemblages of the spring could help and whether its introduction would have any other effects. The BeSs ended up changing the behaviour of the joint significantly. The BeSs bolstered the bolt tension retention considerably, retaining approximately 80% of previous bolt tension under series of severe earthquake loading (Ramhormozian, 2018). However, this inclusion also had another positive effects of of which is improving self-centring behaviour of the joint, and as a result the building. This change made the SHJ an even more viable option when it comes to low-damage seismic resisting connections.

Though the inclusion of the BeSs allowed for better usability of the joint, it also changed aspects of the fundamental behaviour of the connection. This meant the initial hysteresis models developed for the SHJ were inadequate to model the behaviour of the optimised joint under earthquake action. Without accurate modelling, there is a limitation to the extent that the connection can be used throughout the engineering world, if time history analysis is required, thus limiting its usefulness in such case. In aid of this, 22 sets of testing were carried out with this optimised SHJ, all with slightly different materials, surface roughness and shim types (Ramhormozian, 2018). This testing was primarily carried out to ascertain how the optimised joint reacted to these slight changes but could also be used to provide data for an optimised sliding hinge joint hysteresis model. This paper investigates how the current working model of the optimised SHJ was created from one of these experimental data sets and what this model will hold for the future of the connection.

The paper does this by first introducing the subject matter involved in carrying out the project. The mathematical code, the method of its creation and what theory is reinforcing these choices is introduced next. From there the results of the code are visualised to give an idea of the output that has been worked towards throughout the process of the project. The output is then analysed by focusing on the accuracy, the limitations and what can be done in the future. Finally, the paper is closed off by some recommendations and final thoughts.

2 METHODOLOGY

2.1 Outline of methodology

The methodology set out in this section is a general method that has been used to develop hysteretic models for all 22 experimental tests. The method consists of a few steps (shown in figure 1); organize the data points, build up the theoretical behaviour and then plot this data in a digestible form. All these steps were carried out using Microsoft Excel, taking advantage of the functionality and flexibility that the program has when analysing data. Throughout this section, the Glossary of terms for Excel code, presented as an appendix, is used extensively and shows the variables in order of appearance with reference to the excel cells and columns.

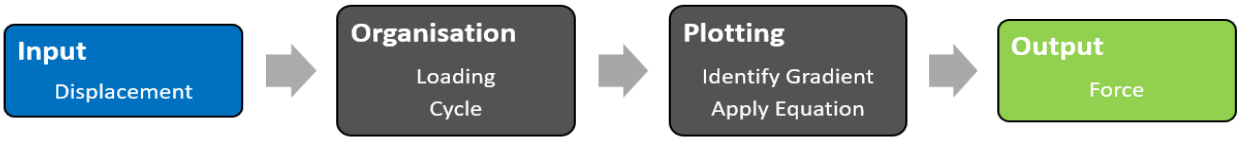

Figure 1: Methodology of Modelling Flow Chart

2.2 Organisation of data

Originally the data sets consisted of 1804 data points with a variety of SHJ data, of which all that was required was the sliding force (kN) and MTS displacement (mm). Using these variables, a hysteresis curve and a sliding force vs time curve could be formed to visualise the data set. In this section the organisation of the Rusted.1a file will be used to explain the organisation that was carried over to all data sets. The first step for this was extracting the earthquake response behaviour by the hinge. For this, the force of time curve was used to identify the periods within the experiment

where the joint was incrementally loaded or unloaded. This was a visually selective process, simply done by extracting the green areas in Figure 1.

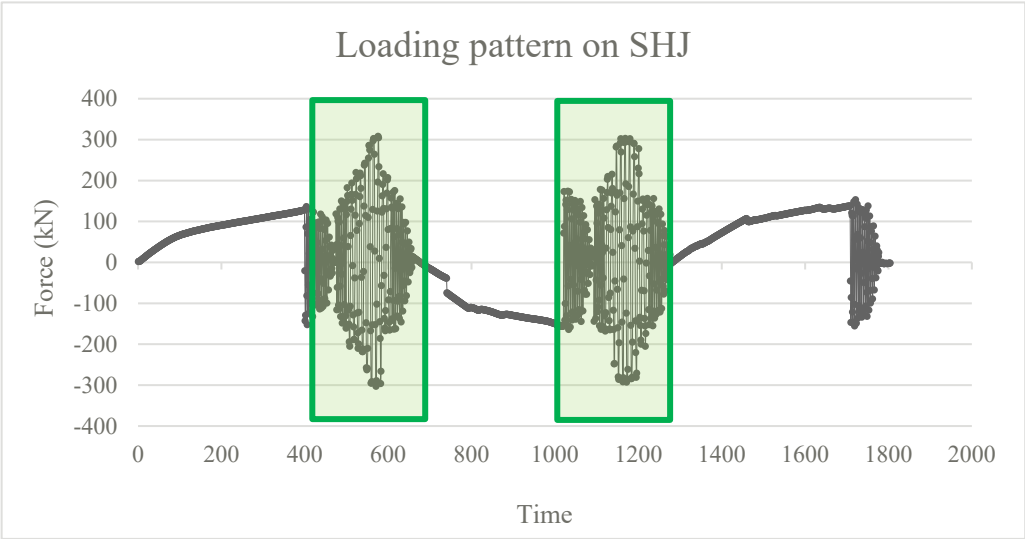

Figure 2: Graph highlighting the areas of earthquake action in a force/displacement graph

From there, all the data had the same behaviour and could be further sorted into the different sections of the hysteretic curve. Using the **D** variable, **Location** and **ΔD** were found using Equation 2.1 and 2.2.

Using these values, the **Loading** variable was developed following a set convention. This consisted of loading and unloading on the left side being negative and positive **ΔD** respectively, the right side being the opposite of this. The **Loading** calculation is shown in Equation 2.

Finally, the last step in organizing the data was to categorize the points into the different behaviours of the sliding hinge joint. It is known that the joint has a varying response to loadings depending on the how far the joint has displaced. This comes down to what part of the SHJ is being engaged by the loading. The first of these behaviours is high cycle loading where the SHJ is in what is called stable sliding. This is where the cap plate is fixed by the bolts which are being pushed in double curvature by the flange, middle and cap plate. It is the most stable and predictable behaviour of the sliding hinge joint as the cap and the bottom plate both slide simultaneously.

The next behaviour is mid cycle loading, this is where stable sliding is not consistently achieved. The bolts in the asymmetric friction joint will just slide between the clearance in their slots, moving only the cap plate as it slides. This behaviour is still predictable and stable. Finally, there is the low cycle. This is not a hysteretic behaviour at all, as the connection is not sliding but is just following the elastic behaviour of the steel that makes up the connection. This is still a predictable behaviour as it approximately follows the steel elastic modulus linearly. With this low cycle behaviour, there is also a transitionary section between it and the mid cycle point. This has been termed a bridge cycle, this behaviour accounts for the unpredictability of the joint movement when it transitions between sliding to and from stationary plate position. As evident by the naming system, each response is activated by certain displacement ranges.

All four of the categories above were differentiated between using the **Cycle** variable. For this, the cyclic behaviours had to be based on the whole cycle which meant the data point alone wasn't enough information so **MAXDForward** and **MAXDBackward** were checked to see which was the best fit. These variables were incorporated by setting a limit for both of 4.1/-4.1mm for the mid cycle, with any values above this being high cycle. For the change between mid and low cycle, **AVGD** had to be less than 1.5mm and the **SUMMAXD** had to be below 4mm for it to be considered a low cycle. The set out of this variable can be seen below in Equation 2.4

The bridge behaviour was also accounted by using Equation 2.5 to convert the first point that changed from mid to low cycle into a bridge cycle point. The visualisation of the hysteretic behaviour for the three separate behaviours can be found in Appendix A.

2.3 Theoretical behaviour

2.3.1 High cycle trend fitting

As stated before, the high cycle is the most predictable behaviour that SHJ offers, making it easy to develop the stiffness gradients. From analysing the data, the simple outline of this cyclic behaviour is shown in Figure 2. With this estimated shape set up, finding the values of all these variables was the next logical step.

The first variables to focus on were **FH0Right** and **FH0Left**. At these high force levels, the SHJ is going in one direction with both friction surfaces sliding. In this state, the bolts display both double curvature and rigid body rotation. The first of these comes down to the effect of the two topping plates (beam flange and cap) not having slotted holes. This means as the middle plate with slotted holes slides, the bolts are pushed across through the middle while still being secured at the top, causing double curvature. Rigid body rotation also occurs at this stage due to BeSs taking some of the pressure from the double curvature by relaxing its conical shape, allowing for rotation of the bolt instead of curvature. These factors combine to create a very low stiffness value, however, due to using high hardness shims (Khoo, Clifton, Butterworth, MacRae, & Ferguson, 2012) the optimised SHJ shows repetitive and predictable stiffnesses across this range. So instead of an increasing stiffness over time, this SHJ has a constant flat gradient. This force level is approximately

300kN for both sides. From further investigation into the average force, it was found that the value was 290kN for **FH0Left** and was 300kN for **FH0Right**. This was determined by the slight directional differences in the SHJ. As it is asymmetrical, the cap plate in one direction will provide significantly more friction due to the deformation of the plate over time. This deformation causes the plate to point along the beam in one direction, adding another surface for friction.

Another important trend was that of **FH1Right** and **FH1Left**. This force value which is the point where **KH1** turns to **KH2** seemed to be at -100kN and 100kN for the right and left side respectively. This is theorized to be the point where the SHJ has changed direction and begins to slide on one of its surfaces, therefore drastically decreasing the stiffness. Before this 100kN/-100kN point, the connection is being unloaded and thus it exhibits the elastic stiffness of the connection which is much higher than that of the sliding joint. This occurs at approximately 100kN as this is where the friction forces for the plate are counteracted, allowing the bolt to start sliding. With the switch point located, the hysteretic trends for the gradients either side of the switch were then deduced from sight. The visual analysis found **KH1** and **KH2** to be approximately 85kN/mm and 14kN/m respectively on both sides.

2.3.2 Mid cycle trend fitting

Much like the high cycle trend, the mid cycle trend is still predictable, having a well set out assortment of stiffnesses. From the mid cycle hysteretic curve in Appendix A, these stiffnesses can easily be sorted into a loading and unloading gradient on each side of the curve. These four stiffnesses are shown approximated in Figure 2, to give an idea of the basic shape of the curve.

The theory behind the mid cycle values is that there is never truly enough displacement to create stable sliding. This means that the cycle is just a less intense version of **KH1** and **KH2** from the high cycle behaviour. Using this, **KM1** and **KM2** were given a less extreme value to their high cycle counterpart; with stiffnesses of 22kN/mm and 58kN/mm respectively.

2.3.3 Low cycle and bridge cycle trend fitting

Unlike the other two behaviours, the low cycle is a bit harder to capture in the model. This is due to the low displacements and forces present throughout its cycles. From looking at the data there seems to be a relatively low stiffness transition which then changes to the relatively higher low stiffness. This transitional stiffness is what is explained previously as the bridge cycle. A graphical representation of the two cycles is shown in Figure 2.

These linear force displacement curves are to the mid cycle what the mid cycle is to the high cycle. Instead of not being able to slide far enough to fully engage the SHJ, during low cycle behaviour, the SHJ is not sliding with either friction surfaces. This means the stiffness is simply the stiffness of the SHJ connection in standard conditions, with minor deviation allow for degradation and other effects. Using these general stiffness definitions, it was found that **KL** and **KB** were 69kN/mm and 50kN/mm respectively.

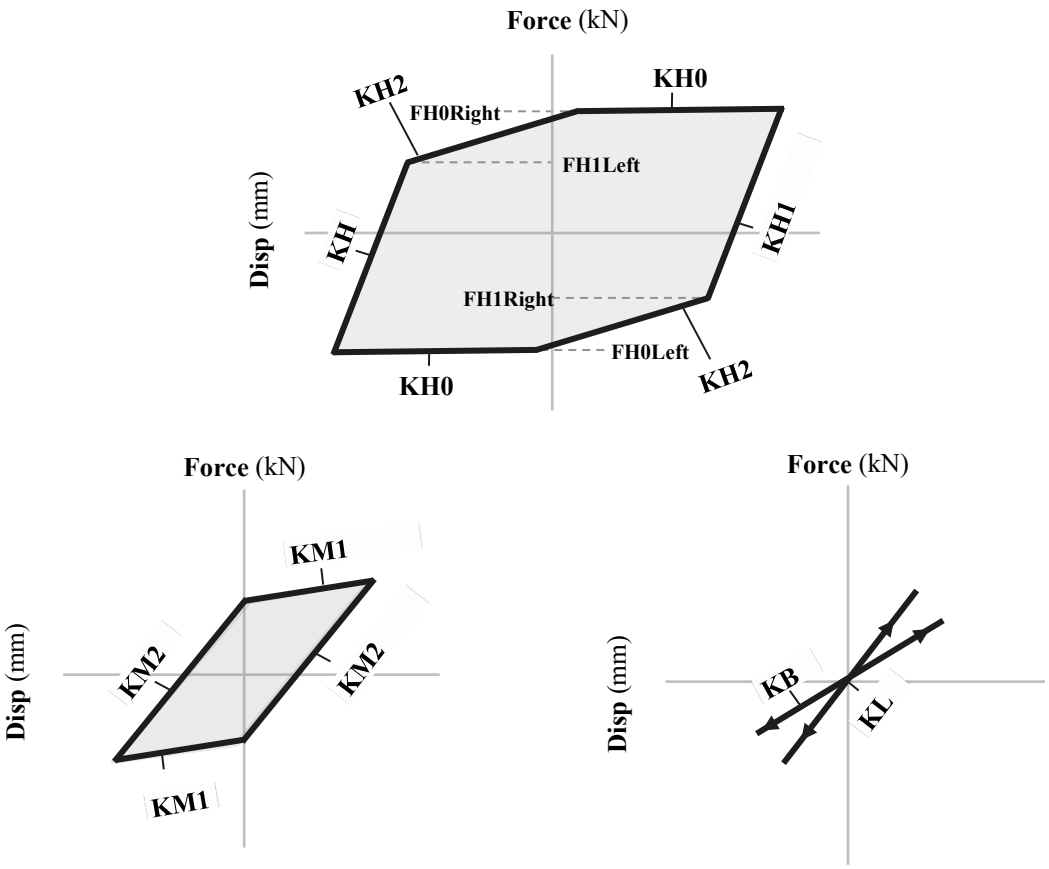

Figure 3: High (top) mid (bottom-left) and low/bridge (bottom right) cyclic hysteretic behaviours of the SHJ

2.4 Recreating data

2.4.1 Introduction

With the stiffness values gathered for the high, mid, low and bridge cyclic behaviours, all that had to be done was to apply these to the data points to achieve a predicted set of forces which could be used to compare to the experimental data to get the accuracy of the model. This was done by a set of equations carried out in excel. These basically followed the same principles:

- Work out new force using stiffness gradient of current position and **ΔD**
- Work out whether this new force crosses over any switches and/or requires re-centring
- Adjust new force if it crosses switch and/or requires re-centring
- Get **FPred** for the point

2.4.2 High cycle

Recreating the high cycle values was more straightforward than the other cycles as the cycle did not require any sort of re-centring. The first two variables to get were **HFPredRight** and **HFPredLeft** which together could be used to work out **HFPredInt**. In addition to these variables, there was also the need for **DHRight** and **DHLeft** that deal with the displacement limit. At 5mm, the curve transitions from **KH2** to **KH0**, reflected in Equation 2.6, for **HFPredRight** with this equation simply mirrored for **HFPredLeft**. These variables then combine to get **HFPredInt.**

Next, both switches at **FH1Left** and **FH1Right** had to be accounted for when **D** went from **KH1** to **KH2**. To do this, the need for the switches; **HSwitch1** and **HSwitch2,** was established, with the former shown in Equation 2.7 the later the negative version of this.

If the switch was needed, **HSwitch1Dist** and **HSwitch2Dist** were calculated by the change in stiffness combined with the predicted force past the switch. The calculations for **HSwitch1Dist** are shown in Equation 2.8.

Finally, **HSwitch1Dist** was combined with **KH2** and added to **FH1Right** to get **HFSwitch1**. The process for which is shown in Equation 2.9 with **HFSwitch2** simply calculated as the negative version of this equation.

2.4.3 Mid cycle

There are three main parts to the plotting of the mid cycle data; predicting force, switching around gradient changes and re-centring the data. Equation 2.10 shows how the first step was done by splitting outcomes into **Location** and **Loading**, to get **MFPred**.

Next, the first switching procedure was taken care of by Equation 2.11 and 2.12, with the second switch just the opposite of this. In the former equation, **MSwitch1** was determined by checking the movement from the previous point. **MFSwitch1** was then established through **MSwitch1** and the use of stiffness gradients.

The final step; re-centring was vital in keeping the reproduction of the hysteretic behaviour on track with the experimental data. Without these, each data point brings a miniscule error which eventually adds together to push the data points far away from where they are required. To carry the re-centring out, first, the code had to work out whether the mid cycle value crossed the y-axis. This was done in either direction to ensure re-centring can occur each cycle consistently. The right to left direction is shown in equation 2.13 and is the opposite of this for the left to right direction.

When a value crossed zero, the force is then reduced as in equation 2.14 to get **MFYIntLow** or **MFYIntHigh.**

The next step was finding the spread of the current hysteresis cycle, this was done by looking back at the **MFYIntLow** and **MFYIntHigh** of the previous 4 points. If there were no viable values for the past four points, the range was simply the current **MFYIntHigh**. This is set out in equation 2.15.

Finally, the data was centred through equation 2.16, essentially halving the **MFYIntRange** and then reducing **MFPredSwitch** by this number.

2.4.4 Low cycle and bridge

Like the cycles before, the low and bridge cycles first require an estimate using the stiffness from decided upon. This step was carried out by equation 2.17 which details the development of **LFPredInt** by using stiffnesses outlined by the **Cycle** variable.

Next, there had to be a check for the need to re-centre, an idea which has been explained in 4.4.3. This check, equation 2.18, was the same check as for the mid cycle but only centred once every time the SHJ was demonstrating low cycle behaviour.

Finally, the predicted force was then either **LFPredInt** or **LFPred**, the later shown as simply the product of **D** and **KL** in equation 2.19.

3 RESULTS

This section covers the outputs of the proposed model. The first part of this, Figure 3, covers the complete reproduction of the hysteretic response under earthquake demand of the Rusted.1a data set. This shows both curves to highlight the similarities of the reproduced and experimental curve.

This section also includes the singular predicted cycles of the SHJ which pertain to maximum displacements of interest. The three displacements thought to show the behaviours best; 3mm, 10mm and 15mm, are shown in Figure 4. These maximum displacement cycles showcase the most important hysteretic behaviours in its simplest state. The curves were created using the equations outlined in section 2.4, adjusted minimally to most accurately create the expected behaviour at these max displacements.

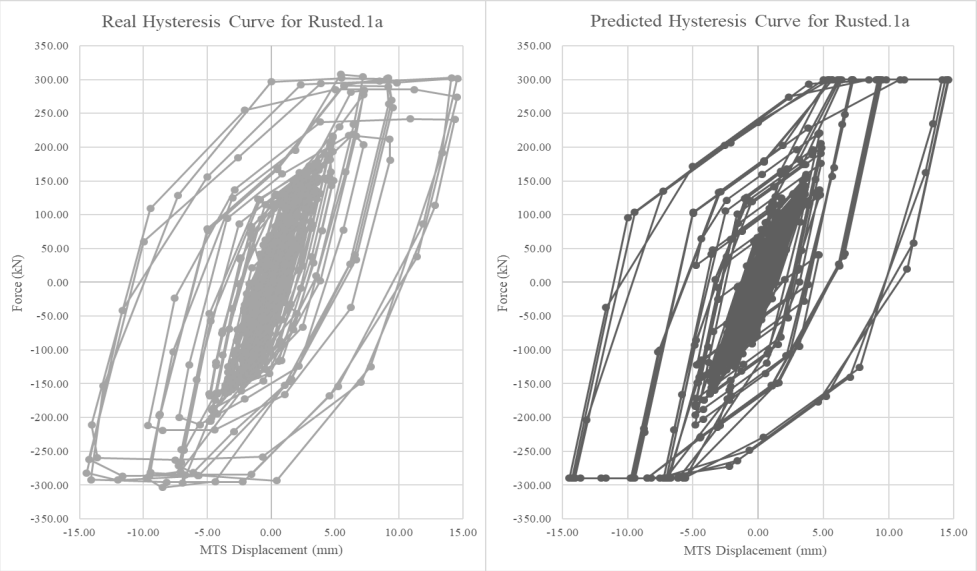

Figure 3: Experimental (left) and predicted (right) from Rusted.1a data set

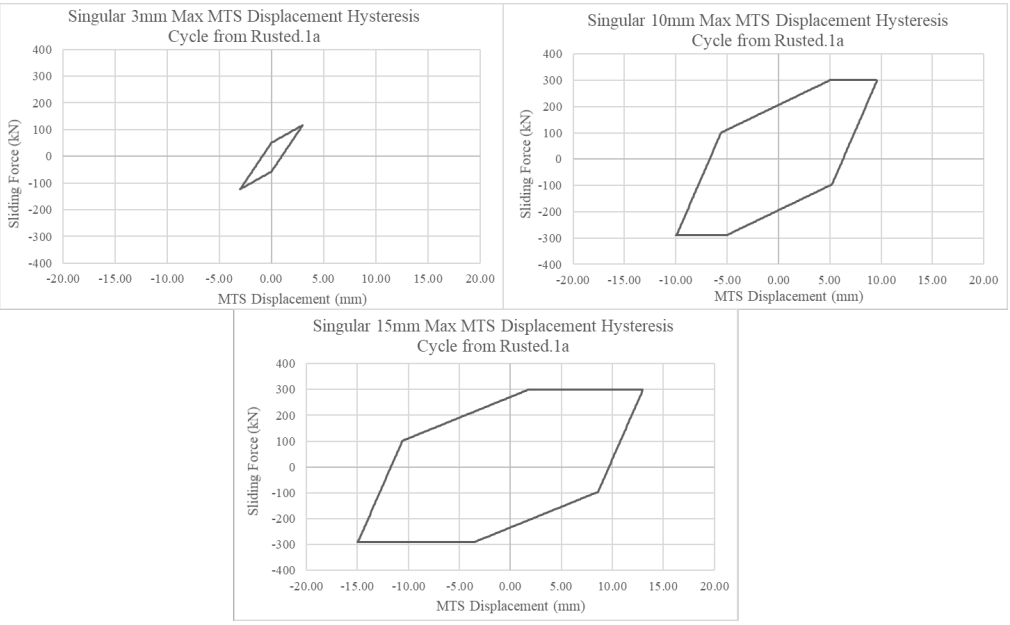

Figure 4: Single predicted curves from the Rusted.1a data set with displacements of 3mm (top-left), 10mm (top-right), 15mm (bottom)

4 DISCUSSION

4.1 Limitations

4.1.1 Low sample rate

The experimental data has influenced the model greatly. One of the slight imperfections of this data is the sample rate that was used while gathering **F** and **D**. The test-rig set-up took 2 measurements per second. Though this makes the data slightly imperfect and more temperamental to model, this does not take away from the validity of the overall trend.

The sample did make it harder to model the corners of the hysteresis curve, this is where most of the modelling issues occurred. The first issue surrounding this area is that there are not many data points. This issue is intensified when the hysteresis goes around the corner shown in Figure 5, transitioning from the KH0 gradient into the KH1 gradient. In this area, the code is unable to find the exact point where the stable sliding terminates, and the unloading begins. This means that though the gradients match up with the experimental data, they are not a perfect representation of the stiffness that occurs at these points.

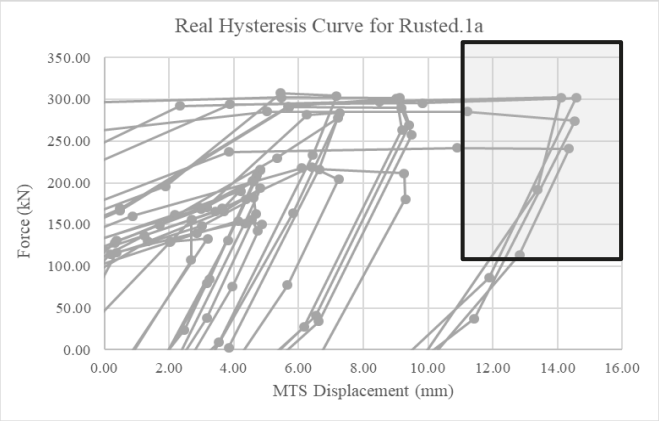

Figure 5: Experimental data showing the issue of data points going around the corner

4.1.2 Linear point connection

Choosing to develop this system in excel has meant that the movement from point to point must be in a linear fashion. This is down to the lack of capability for the program to plot accurate non-linear curves between sets of data points which is compounded by the low sample rate the data set was created with. In the actual connection, it is expected that the displacement would not interact linearly with the force as it was loaded and unloaded.

4.1.3 Range limitations

Using Microsoft Excel was extremely useful for the development of this paper's model; however, it did set some limitations for our model. This main issue here was that ranges were required for the certain cyclic and loading behaviours. This meant that values that were at the extremities of the ranges had to be lumped into one part or the other. In most cases, the code was intelligent enough to put these values in the right categories but in some instances, these were categorized incorrectly. Within the terms of the entire set of the data, these are impossible to recognize and the only way to truly pick up these instances is to take each cycle individually. This would require a very intensive system which could not be created in excel within the time frame for this project.

4.2 Accuracy and validity of results

4.2.1 Overall trends

Looking at all the data points together, the trends of the experimental and the predicted match to a high degree. In terms of calculating how close the numbers matched, the process was not overcomplicated and is as follows. First **Diff** was found for each variable and then the **Error** for each point was found as a percentage max cycle value from the **Location**. The equation for these error values can be found in equation 4.1.

Finally, these errors were added up in **CumError** to get the **TotalError**. For the Rusted.1a data set the **TotalError** was 9.3%, which is not a huge error with close to 600 data points.

4.2.2 High cycle trends

In terms of the individual cycles, it is more advantageous to look at the accuracy of how the shape was achieved and the visual likeness than to use a singular error percentage as above. Firstly, as explained before, the high cycle very much followed the behaviour that the theory predicted which adds validity to the high cycle model. In addition to this, the cycle has a close visual relationship to the experimental data which is shown by Figure 6 and the high cycle experimental curve in Appendix A. The exterior backbone at the extremity decreasing to the bulk of the data points orbiting the origin point are common visual points between the two curves.

4.2.3 Mid cycle trends

The mid cycle, much like the high cycle, achieves validity through exhibiting many traits which are attributed to the theoretical behaviour of the SHJ. Though this model reproduces the experimental most of the time, there is one lapse in this. This seems to be an instance where the re-centring set in place by the code has not worked correctly. This could also plausibly be a major outlier which could be removed. Either way, this curve still requires some work on the minor details.

4.2.4 Low cycle trends

The low cycle behaviour was the hardest of the three behaviours to execute at a high level of accuracy. This was mainly down to the reliance on the re-centring capability of the code. The low cycle is so reliant on this due to its largely continuous gradient throughout all the cycles. Any minor errors off this gradient, show up blatantly and are magnified the longer they go un-centred. This can be seen by a few points in Figure 6, which look largely out of place in terms of the entire cyclic behaviour. These are instances where the re-centring hasn't worked the way it is supposed to or one outlier has thrown the whole data out of order for a few data points. The instances were troubleshooted as best as possible, but some slipped through. Though not ideal the errors must also be taken with a grain of salt because of the small displacements and forces this cyclic behaviour operates at there are bound to be considerable outliers. However, this still points to a need for more refining of this code to make it more of an accurate representation.

In terms of the theory behind this cyclic behaviour, it is not a strictly theorized cyclic behaviour of the SHJ but does follow the loose elastic behaviour that is normally present at low displacements and forces.

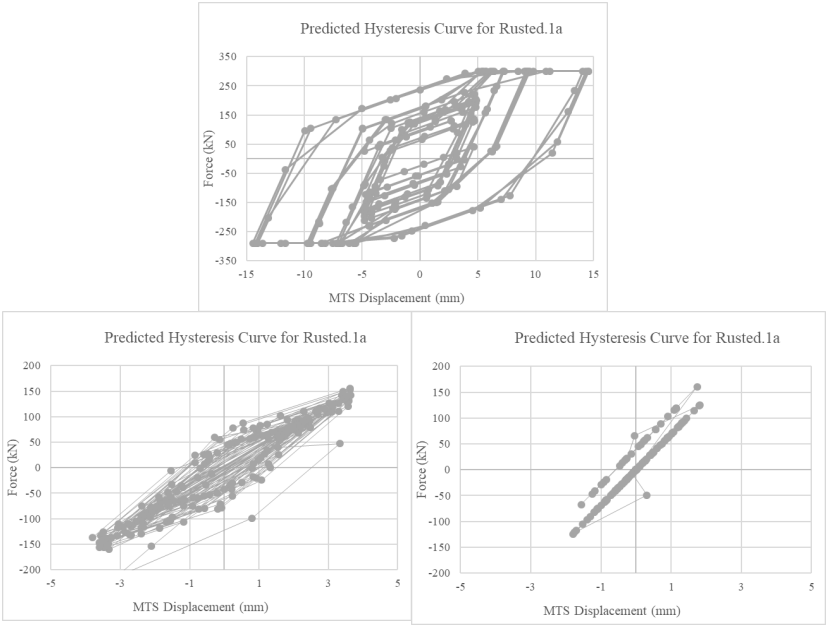

Figure 6: Individual Cyclic Behaviour for high (top), mid (bottom-right) and low (bottom-left)

4.3 Improvements and recommendations

4.3.1 Increased sample rate and experiments

Increasing the sample rate would have made allowed for a greater accuracy to be achieved in the final model. As stated previously, this does not take away from the encompassing model as this would still be the same. However, being able to get a sample rate of just 0.1 seconds would have made a difference to the data available for both seeing the trends and for accuracy purposes.

4.3.2 Incorporation into structural modelling software

As a recommendation to future projects would be to translate the code explained above into some form of programming language (Microsoft Visual Basic or C++). From there the code could easily be imported into whatever the most accessible structural analysis software. This would make the properties and behaviours of the optimised SHJ available for design in software making the connection a lot more accessible for engineers in New Zealand and across the world.

4.3.3 Statistical Analysis

Though currently there is a form of statistical analysis integrated into the code explained above with the use of **TotalError**. However, this is not the most strict and accurate way of measuring whether the switches and gradients decided upon for the model are a good fit. To truly get statistical proof that the values were correct to a certain degree would be to use a true statistical method not only on the Rusted.1a data set but also on the 22 other data sets. This would give a truer and more informed idea of the gradients and switches.

5 CONCLUSIONS

Detailed in this paper is the creation of a completely new model for the optimised sliding hinge joint with asymmetric friction connections in Microsoft Excel. This model can currently reproduce the behaviour in the Rusted.1a data set within 9.6% indicating that it can carry out its function as a model. This model is also able to create representative curves for three max connection displacements. It is expected that this research may help to give a great understanding of the optimised connection and provide a framework for use in structural modelling software.

REFERENCES

Engelhardt, M. D. (2001). Ductile detailing of steel moment frames: Basic concepts, recent developments and unresolved issues. Paper presented at the Proceedings, XIII Mexican Conference on Earthquake Engineering,

Hamburger, R. O., & Frank, K. (November 1994). Performance of welded steel moment connections - issues related to materials and mechanical properties. Paper presented at the Sac 94-01, 69-78.

Khoo, H., Clifton, G. C., Butterworth, J., MacRae, G. A., & Ferguson, G. (2012). Influence of steel shim hardness on the sliding hinge joint performance. Journal of Constructional Steel Research, 72, 119-129. doi:10.1016/j.jcsr.2011.11.009

MacRae, G., Clifton, C., & Innovations, S. (2013). Low damage design of steel structures. Paper presented at the Steel Innovations 2013 Workshop, Christchurch, New Zealand,

Ramhormozian, S. (2018). Enhancement of the sliding hinge joint connection with belleville springs

Ramhormozian, S., Clifton, G. C., MacRae, G. A., Davet, G. P., & Khoo, H. (2019). Experimental studies on belleville springs use in the sliding hinge joint connection. Journal of Constructional Steel Research, 159, 81-94. doi:10.1016/j.jcsr.2019.03.031

APPENDIX A: NOTATION LIST

Variable	Description	Row/Cell
D	MTS displacement from SHJ experimental testing (mm)	A, AF
F	Sliding force from SHJ experimental testing (kN)	
Location	Whether the specific point is on the right or left of the hysteretic curve	AG
ΔD	Change in **D** from the previous point	AH
Loading	Whether the point is in a loading or unloading section of the hysteretic cycle	AI, C
Cycle	Determines the cyclic (high, mid, low or bridge) behaviour through **D** of surrounding points	AO, AP, AQ
MAXDForward	Max **D** of six forward looking points (mm)	AL
MAXDBackward	Max **D** of six previous points (mm)	AM
AVGD	Average **D** between the previous and forward-looking point (mm)	AK
SUMMAXD	Sum of **MAXDForward** and **MAXDBackward** (mm)	AN
FH0Right	Force at which **KH0Right** occurs at high cycle (kN)	D3
FH0Left	Force at which **KH0Left** occurs at high cycle (kN)	D7
KH0	Backbone stiffness value for the SHJ at high cycle (kN/mm)	N/A
FH1Right	Force at which **KH1** changes to **KH2** on the right side of the hysteresis curve at high cycle(kN)	D20
FH1Left	Force at which **KH1** changes to **KH2** on the left side of the hysteresis curve at high cycle (kN)	D21
KH1	Stiffness value for the first unloading gradient at high cycle (kN/mm)	D4, D8,

KH2	Stiffness value for the second unloading gradient at high cycle (kN/mn)	D2, D5, D6, D9
KM1	Stiffness gradient of the loading sections of the hysteresis curve at mid cycle (kN/mm)	D10, D12
KM2	Stiffness gradient of the unloading sections of the hysteresis curve at mid cycle (kN/mn)	D11, D13
KL	Stiffness gradient of the hysteresis curve at low cycle (kN/mn)	D14
KB	Stiffness gradient of the hysteresis curve at bridge cycle (kN/mn)	D15
FPred	Force predicted from the excel code (kN)	D, BU
DHRight	Displacement along the hysteresis curve at which **FH0Right** occurs (mm)	D18
DHLeft	Displacement along the hysteresis curve at which **FH0Left** occurs (mm)	D19
HFPredInt	Force predicted from the excel code for high cycle before switches (kN)	AT
HFPredRight	Predicts the change in high cycle force or lack thereof on the right side of the hysteresis for a point before switches (kN)	AR
HFPredLeft	Predicts the change in high cycle force or lack thereof on the right side of the hysteresis for a point before switches (kN)	AS
HFPred	Force predicted from the excel code for high cycle (kN)	BA, BB
HSwitch1	Checks whether a point changes between **KS1** and **KS2** and needs adjustment on the left side of the hysteresis	AU
HSwitch1Dist	Calculates real distance that the point travels past **FH1** from **HFPredLeft**	AV
HFSwitch1	Calculates real force using **Switch1Dist** and **KS2** (kN)	AW
HSwitch2	Checks whether a point changes between **KS1** and **KS2** and needs adjustment on the right side of the hysteresis	AX
HSwitch2Dist	Calculates real distance that the point travels past **FH1** from **HFPredRight**	AY
HFSwitch2	Calculates real force using **Switch1Dist** and **KS2** (kN)	AZ
MFPred	Initial force predicted from the excel code for low cycle before switches and re-centering are applied (kN)	BC
MSwitch1	The distance the point has moved past switch1 (0 if it hasn’t) (mm)	BD
MFSwitch1	The force change from both the distance before switch1 and **LSwitch1** (kN)	BE
MSwitch2	The distance the point has moved past switch 2 (0 if it hasn’t) (mm)	BF
MFSwitch2	The force change from both the distance before switch 2 and **LSwitch2** (kN)	BG
MFPredSwitch	Initial force predicted from the excel code for mid cycle before re-centering is applied (kN)	BH

MYIntLow	Whether the **D** has crossed zero from the previous **D** at negative force	BI
MFYIntLow	The negative **F** at which the point crosses zero in low cycle (kN)	BJ
MYIntHigh	Whether the **D** has crossed zero from the previous **D** at positive force	BK
MFYInthigh	The positive **F** at which the point crosses zero in mid cycle (kN)	BL
MFPredCent	The final **F** prediction for mis cycle which includes switches and re-centring (kN)	BO
LFPredInt	The initial **F** estimate based on **KL** (kN)	BR
LCent	Checks whether the point requires re-centring in low cycle	BS
LFPred	Predicts **F** from low cycle with re-centring applied (kN)	BT
ABSDiff	Difference between **force** and **PredForce** (kN)	E
Error	**ABSDiff** / (**FH0Right** + **FH0Left**) *100 (%)	F
CumError	Average of all previous points **Error** (%)	G
TotalError	Final **CumError** point	D24

APPENDIX B: CODE EQUATIONS

Location = *IF(**D** > 0,"Right", "Left")* (2.1)

Δ***D*** = ***D****(previous)* - ***D*** (2.2)

Loading = *IF(OR(AND(**Location** = "Right", Δ**D** > 0), (AND(**Location** = "Left", Δ**D** < 0))), "Loading", "Unloading")* (2.3)

Cycle = *IF(OR(**MAXDForward** > 4.1, **MAXDBackward** > 4.1), "High", IF(AND(**AVGD** < 1.5, **SUMMAXD** < 4),"Low", "Mid"))* (2.4)

Cycle = *IF(AND(**Loading** = "Mid", **Loading****(previous)** = "Low"),"Bridge", **Loading**)* (2.5)

HFPredRight = *IF(OR(**Cycle** = "Mid", **Cycle** = "Low", **Cycle** = "Bridge"), "not in high cycle", IF(**Location** = "Right", IF(**Loading** = "Loading", IF(**D** < **DHRight**, **FPred****(previous)** + (**D** * **KH2**), **FH0Right**), IF(**HFPred** > **FH1Right**, **PredF****(previous)** + (**D** * **KH1**), **FPred****(previous)** + (**D** * **KH1**))), "0"))* (2.6)

HSwitch1 = *IF(**HFPredRight** = "not in high cycle", "not in high cycle", IF(AND (**Location** = "Left", **Loading** = "Unloading", **HFPredInt** > **FH1Left**, **HFPred****(previous)** < **FH1Left**), "yes", "no"))* (2.7)

HSwitch1Dist = *IF(**HFPredRight** = "not in high cycle", "not in high cycle", IF(**HSwitch1** = "yes", ((Δ**D** / (**HFPredInt** - **HFPred****(previous)**) * (**HFPredInt** - **FH1Left**))), 0))* (2.8)

HFSwitch1 = *IF(**HFPredRight** = "not in high cycle", "not in high cycle", IF(**HSwitch1** = "no", 0, (100 + (**HSwitch1Dist** * **KH2**))))* (2.9)

MFPred = *IF(**Cycle** = "Mid", IF(**Cycle** = "Mid", IF(**Location** = "Right", IF(**Loading** = "Loading", **FPred****(previous)** + (**ΔD** * **KM1**), **FPred** (previous) + (**ΔD** * **KM2**)), IF(**Loading** = "Loading", **FPred** (previous) + (**ΔD** * **KM1**), **FPred** (previous) + (**ΔD** * **KM2**))), IF(**Cycle** = "Low", **FPred** (previous) + (**ΔD** * **KL**), **FPred** (previous) + (**ΔD** * **KB**))), 0)* (2.10)

MSwitch1 = *IF(OR(**Cycle** = "Low", **Cycle** = "High"), 0, IF(AND(**D** < 0, **D****(previous)** > 0), **D**, 0* (2.11)

MFSwitch1 =*IF(**MSwitch1** < 0, **FPred****(previous)** + (**ΔD** * **KM2**)+(**ΔD** * **KM1**), 0)* (2.12)

MYIntLow = *IF (**Cycle** = "Mid", IF(AND(**D** < 0, **D** > 0) ,"it crosses 0", "it does not cross 0"), "not in mid cycle")* (2.13)

MFYIntLow = *IF(**MYIntLow** = "it crosses 0", (**MFPredSwitch** - (**D** * **KM1**)), 0)* (2.14)

MFYIntRange = *IF(**MYIntLow** = "it crosses 0", IF(**MFYIntLow** = 0, IF(**MFYIntLow****(previous)** = 0, IF(**MFYIntLow****(2 previous)** = 0, IF(**MFYIntLow****(3 previous)** = 0, IF(**MFYIntLow****(4 previous)** = 0, **MFYIntHigh**, **MFYIntHigh**+ **MFYIntLow****(4 previous)**), **MFYIntHigh** + **MFYIntLow****(3 previous)**), **MFYIntHigh** + **MFYIntLow****(2 previous)**), **MFYIntHigh** + **MFYIntLow****(previous)**), 0) ,0)* (2.15)

MFPredCent =*IF(**MCent** = "yes", IF(**MFYIntRange** < -30, **MFPredSwitch** - (**MFYIntRange** / 2), **MFPredSwitch** - (**MFYIntRange** / 2), **MFPredSwitch**)* (2.16)

LFPredInt = *IF(**Cycle** = "Low", **FPred****(previous)** + (**ΔD** * **KL**), IF(**Cycle** = "Bridge", **FPred****(previous)** + (**ΔD** * **KB**), 0))* (2.17)

LCent *=IF(* ***LPred*** *= "not low", "not low", IF(* ***LCent****(previous) = "reset", "reset", IF(* ***LCent****(previous) = "recentre", "reset", IF(OR(AND(* ***D****(previous) < 0,* ***D*** *> 0), AND(* ***D****(previous) > 0,* ***D*** *< 0)), "recentre", 0))))* (2.18)

LFPred *= IF(* ***LPred****="not low", "not low", IF(* ***LYInt*** *= "recentre",* ***D*** ** **KL**, 0))* (2.19)

Error *= (* ***Diff*** */ (IF(* ***FPred*** *> 0,* ***FH0Right****,* ***FH0Left*** *)) * 100)* (4.1)